Talanta 271 (2024) 125712

Contents lists available at ScienceDirect

Talanta

journal homepage: www.elsevier.com/locate/talanta

# Non-matrix-matched calibration in bulk multi-element laser ablation – Inductively coupled plasma – Mass spectrometry analysis of diverse materials

Kristina Mervič [a,b], Vid S. Šelih [a], Martin Šala [a,*], Johannes T. van Elteren [a,**]

[a] Department of Analytical Chemistry, National Institute of Chemistry, Hajdrihova 19, 1000, Ljubljana, Slovenia
[b] Jožef Stefan International Postgraduate School, Jamova Cesta 39, SI-1000, Ljubljana, Slovenia

ARTICLE INFO

Handling editor: J. Wang

ABSTRACT

Laser ablation inductively coupled plasma - mass spectrometry (LA-ICP-MS) is a frequently used microanalytical technique in elemental analysis of solid samples. In most instances the use of matrix-matched calibration standards is necessary for the accurate determination of elemental concentrations. However, the main drawback of this approach is the limited availability of certified reference materials. Here, we present a novel conceptual framework in LA-ICP-MS quantification without the use of matrix-matched calibration standards but instead employment of an ablation volume-normalization method (via measurement of post-ablation line scan volumes by optical profilometry) in combination with a matrix-adapted fluence (slightly above the ablation threshold). This method was validated by cross-matrix quantification of reference materials typically investigated by LA-ICP-MS, including geological and biological materials. This allows for more accurate and precise multi-element quantification, and enables quantification of previously unquantifiable elements/materials.

## 1. Introduction

Laser ablation inductively coupled plasma mass spectrometry (LA-ICP-MS) is a surface microanalytical technique that provides spatially resolved information on the distribution of major, minor, and trace elements. It enables direct analysis of solid materials with high detection performance and lateral resolution in the order of micrometers for large sample areas. Because of the qualitative and quantitative capabilities of the technique, the minimal sample preparation requirements, and major cell/instrumentation improvements and data processing developments, LA-ICP-MS is now used in a wide variety of fields (geology, archaeology, mineralogy, materials studies, forensics, environmental research, medicine, and biology) [1–9].

In recent years, development of fast washout cells enabled rapid analysis by shortening the single pulse response down to 1 ms or even below [10], and thus much faster mapping compared to conventional systems where a typical single pulse response was approximately 500 ms, depending on the instrument, resulting in either mapping of larger areas or the application of smaller spot sizes without increasing experiment time. In addition, rapid aerosol transport allows for much higher sample throughput, resulting in higher signals and consequently improving the signal-to-noise ratio, i.e., achieving better sensitivity [11–13]. In recent years, significant improvements in instrument hardware, combined with a better understanding of the effects of operating conditions on image quality, have made LA-ICP-MS mapping not only faster, but also much more powerful. Advancements in laser ablation parameter optimization to avoid mapping artefacts such as smearing, noise, blurring, and aliasing, are yielding high quality 2D LA-ICP-MS (multi)element maps [14–16]. The use of recently introduced ICP-time-of-flight (TOF)-MS instruments has pushed the technique even further. Compared to the commonly used sequential quadrupole mass analyzers, ICP-TOFMS provides quasi-simultaneous analysis of the entire elemental mass spectrum. Several applications of ICP-TOF-MS have been described, from thin biological tissue samples to meteorites. The combination of laser ablation with ICP-TOF-MS has proven to be a powerful tool for comprehensive sample characterization, allowing simultaneous detection of ions over the entire elemental $m/z$ range with very low sample consumption [12,17–20].

Despite the tremendous progress made in LA-ICP-MS analysis, primarily leading to faster surface element mapping, calibration still proves

* Corresponding author.
** Corresponding author.
*E-mail addresses:* martin.sala@ki.si (M. Šala), elteren@ki.si (J.T. van Elteren).

https://doi.org/10.1016/j.talanta.2024.125712
Received 13 November 2023; Received in revised form 11 January 2024; Accepted 22 January 2024
Available online 1 February 2024

**Table 1**
Specification of the standard materials used in this non-matrix-matched LA-ICP-MS calibration study.

| Standard | Material type | Nominal concentration | Density | |
|---|---|---|---|---|
| In-house prepared gelatin standards [16] | 10 % (m/V) porcine-skin gelatin, type A, bloom strength 300 | ~10–250 μg $g^{-1}$ | 1.35 g $cm^{-3}$[a] | Sigma-Aldrich, St. Louis, MO, USA |
| NIST SRM 614 | Silicate glass | ~5 μg $g^{-1}$ | 2.57 g $cm^{-3}$[a] | National Institute for Standards and Technology, Gaithersburg, MD, USA |
| NIST SRM 612 | Silicate glass | ~50 μg $g^{-1}$ | 2.52 g $cm^{-3}$[a] | |
| NIST SRM 610 | Silicate glass | ~500 μg $g^{-1}$ | 2.52 g $cm^{-3}$[a] | |
| Corning Museum of Glass (CMG-B) | Silicate glass synthetic glass replicating ancient compositions | / | 2.60 g $cm^{-3}$[a] | Corning Museum of Glass, Corning, NY, USA |
| GSJ CRM JCp-1 Coral (*Porites* sp.) | Carbonate material | / | 2.0 g $cm^{-3}$[b] | myStandards GmbH, Kiel, Germany |
| GSJ CRM JCt-1 Giant Clam (*Tridacna gigas*) | Carbonate material | / | 2.0 g $cm^{-3}$[b] | |
| NIST SRM 1547 Peach leaves | Botanical material | / | 1.65 g $cm^{-3}$[a] | National Institute for Standards and Technology, Gaithersburg, MD, USA |
| Plešovice | Zircon mineral | | 4.60 g $cm^{-3}$[c] | |
| DLH-8 | Silicate glass | ~150 μg $g^{-1}$ | 2.65 g $cm^{-3}$[a] | P&H Developments Ltd. |

[a] Measured with a gas pycnometer.
[b] Calculated based on their composition via approximation of their structure and main component.
[c] Gathered from a known source [34].

to be a challenging matter due to matrix effects, unless there is a harmonization of the matrix composition between the sample and the calibration standard(s). Differences in the properties of the matrices analyzed, e.g., absorptivity, reflectivity, thermal conductivity, etc., may lead to differences in ablation rate (mass or volume of material ablated), particle size distribution, particle transport in the interface and their vaporization, atomization and ionization in the ICP [21,22]. This can lead to elemental fractionation, wherein the signals detected for different elements do not accurately reflect the composition of the ablated matrix. Consequently, this can significantly disrupt the calibration process [23,24].

As in most instances matrix-matching is the preferred choice to avoid calibration issues, in practice suitable certified standard materials are not always available, especially for biological, environmental, and medical samples. To this end, several in-house produced standard materials have been developed that closely resemble certain samples [25,26]. One of these are gelatin gels, which have proven to be excellent multielement matrix-matched standards for biological samples due to their very similar matrix behavior upon laser ablation [27–29], ease of preparation and the possibility of adjusting the concentration range [30,31]. However, finding suitable standards is a problem for other types of samples than proteinaceous samples, especially in geology, where LA-ICP-MS is widely used. In order to have suitable matrix-matched standards, there would have to be a homogeneous standard for each mineral species, which is a practical impossibility. Alternatively, nano-particulate pressed powder pellets are made either from naturally occurring minerals or pre-existing CRMs for LA-ICP-MS analysis [32]. Nonetheless, micro-standards are powdered, compressed materials that might not have the same ablation properties as the mineral samples.

This work will focus on a procedure based on non-matrix-matched calibration via ablation volume-normalization, where the LA-ICP-MS signals are normalized to the ablated volume (or mass when matrix densities are known or measurable), thereby correcting for potential ablation rate differences between sample and calibration standard. A variety of materials (several glasses, carbonates, gelatin, as well as plant and zircon material) was studied, including “hard” and “soft” materials, to act as both sample and calibration standard via cross-calibrating each material against every other material in bulk analysis mode.

## 2. Experimental section

### 2.1. Materials and standards

LA-ICP-MS experiments were performed using ten different standard materials with widely varying matrix properties, either custom-prepared or commercially available (Table 1): i) an in-house prepared gelatin gel [30], often used as the “standard of choice” for calibration of biological material as their matrix is very similar to that of biological samples [29,31], containing nine elements (As, Be, Co, Cr, Fe, Mn, Ni, Pb and Sr) in the concentration range 10–250 μg $g^{-1}$; ii) three frequently used multielement National Institute of Standards (NIST) glass standards with nominal concentrations of ca. 500 μg $g^{-1}$ (NIST 610), ca. 50 μg $g^{-1}$ (NIST 612), and ca. 5 μg $g^{-1}$ (NIST 614); iii) a Corning Museum of Glass (CMG) standard mimicking historic compositions (CMG-B); iv) a modern synthetic glass from P&H Developments Ltd. (DLH-8); v) two carbonate materials (myStandards GmbH)) originating from coral (JCp-1, *Porites* sp., Geological Survey of Japan, GSJ) and giant clam (JCt-1, *Tridacna gigas,* Geological Survey of Japan, GSJ), and commonly used in geochronology; vi) a zircon often used as a quality control in geological studies (Plešovice) [33]; and vii) a plant material from ground peach leaves (NIST 1547) subjected to pressed powder pelletizing yielding a ca. 3 mm thick pellet.

Certified values for the commercial standard materials (NIST and GSJ) are available from their Certificate of Analysis (COA), mostly giving average element concentrations with an expanded uncertainty, which were recalculated to averages with a standard deviation. For the non-certified materials or elements, average element concentrations and their variability were determined by unweighted averaging of the element concentrations obtained from the GeoReM database (http://georem.mpch-mainz.gwdg.de) as weighted averaging was impossible due to the non-consistent nature of the reported associated uncertainties.

Reported densities of the materials in Table 1 were either known or measured (see section 2.2). The ten materials were used as both calibration standards and samples in cross-matrix quantification experiments, mostly based on one-point calibration. However, also multi-point calibration was performed using the NIST 61X SRM glasses for several certified element concentrations, and the gelatin gels with custom-selected element concentrations.

### 2.2. Instrumentation and measurement

Experiments were performed with an Analyte G2 193 nm ArF* excimer laser ablation system (Teledyne Photon Machines Inc., Bozeman, MT) equipped with a standard two-volume ablation cell (HelEx II). The LA system was connected to a quadrupole ICP-MS instrument (Agilent 7900x, Agilent Technologies, Santa Clara, CA, USA) via the Aerosol Rapid Introduction System (ARIS) coupled to the LA Adaptor Assembly glass expansion unit (Glass Expansion Inc., Pocasset, MA), a long-pulse module with a total aerosol particle washout time of approximately 100 ms. The LA-ICP-MS multi-element analysis

**Table 2**
Operational LA-ICP-MS conditions used for multielement mapping of the 10 different samples (standard materials).[a]

| LA (Analyte G2, ARIS, and glass expansion unit) | |
|---|---|
| Wavelength (nm) | 193 |
| Laser fluence (J cm$^{-2}$) | −0.5 (gelatin)<br>−1.0 (NIST SRM 1547 Peach leaves)<br>−3.6 (NIST SRM 610/612/614, CMG-B, DLH-8, Plešovice, JCt-1, JCp-1) |
| Repetition rate (Hz) | 100 |
| Scanning mode | Line scanning |
| Dosage (shots per pixel) | 10 |
| Washout time (ms) | ca. 100 |
| Beam size (μm) | 10 |
| Mask shape | Square |
| He carrier flow rate (L min$^{-1}$) cup\|cell | 0.3\|0.3 |
| **ICP-MS (Agilent 7900x)** | |
| $R_f$ power (W) | 1500 |
| Plasma gas flow rate (L min$^{-1}$) | 15 |
| Auxiliary gas flow rate (L min$^{-1}$) | 0.9 |
| Ar makeup flow rate (L min$^{-1}$) | 0.8 |
| Data acquisition | Time-resolved |
| Dwell time (ms) | 8.5 ($^{9}$Be,$^{52}$Cr)<br>9.0 ($^{54}$Co,$^{55}$Mn,$^{56}$Fe,$^{60}$Ni,$^{75}$As,$^{88}$Sr,$^{208}$Pb) |
| Acquistion time (ms) | 100 |
| Nuclides measured | $^{9}$Be,$^{52}$Cr,$^{54}$Co,$^{55}$Mn,$^{56}$Fe,$^{60}$Ni,$^{75}$As,$^{88}$Sr,$^{208}$Pb |

[a] To mitigate the signal drift effects, sensitivity, and reproducibility on different days or measurement rounds, the advancements in optimizing parameters for the best image quality in LA-ICP-MS, were implemented.A 3D optical interference microscope (Zegage PRO HR, Zygo Corporation, Middlefield, CT) was used to determine the ablation volumes of the ablated line scans in samples and standards. The 3D information was recorded using a 50 × magnification objective lens with a lateral resolution of 0.173 μm and a surface topography repeatability of ≤3.5 nm. Since all the samples and standards involved were flat and smooth, it was not necessary to measure the initial pre-ablation surface morphology.

conditions for different (standard) materials in line scan mode are listed in Table 2. In contrast to matrix-matched calibration where a fixed fluence is used, in this work fluences were selected just above the matrix-dependent ablation threshold where the highest signal-to-noise ratio is observed [35], and the most accurate concentration values are obtained. Each LA-ICP-MS analysis was based on five replicate line scans on both the sample and standard, followed by subtraction of the elemental gas blank, and processing of the data according to section 3.2.

As calibration via ablation-volume normalization results in mass/volume concentrations (μg cm$^{-3}$), to convert to mass/mass concentrations (μg g$^{-1}$), densities of materials (g cm$^{-3}$) should be available. Densities of NIST 610, NIST 612, NIST 614, CMG-B, NIST 1547 pellet, DLH-8, and gelatin gels were measured using a helium gas pycnometer (1345 AccuPyc II, Micromeritics, Norcross, GA). The density of the materials GSJ JCp-1, and GSJ CRM JCt-1 were calculated based on their composition via approximation of their structure and main components, whereas for the Plešovice material the density was available from known sources [34].

### 2.3. Data processing software

ImageJ (National Institute of Health, USA), OriginLab (OriginPro 2018, OriginLab Corporation, Northampton, MA, USA) and RStudio (R version 4.1.0, 2021, The R Foundation for Statistical Computing) software packages were used for data processing of element data. The surface topography data were processed using Mx™ software (v. 8.0.0.23, Zygo Corporation, Middlefield, CT), followed by conversion to csv files in MatLab R2020a (MathWorks).

## 3. Results and discussion

### 3.1. Matrix-dependent material removal upon LA

Depending on the properties of the matrix and its coupling with the laser beam, the amount of material ablated per laser spot differs significantly for different materials, under the same laser pulse energy. This is illustrated in Fig. 1, where it can be seen that the amount of material ablated with the same laser fluence can vary by as much as 5.4 times (for the gelatin: NIST 610 crater volume ratio), which is why using different material types for standard and sample will not give accurate results if the ablated volume is not considered. This underscores the potential inaccuracy of results when employing diverse material types for the standard and sample, unless the ablated volume is accounted for or matrix compatibility is ensured.

### 3.2. Non-matrix-matched calibration via ablation volume-normalization

To perform non-matrix-matched calibration via ablation volume-normalization, line scan volumes in samples and calibration standards were measured by optical interference profilometry. Even though this method solely addresses discrepancies in ablation rates within matrices, and does not account for variations in particle size distribution, the transport of particles to the ICP, and their ionization within the plasma, we will demonstrate that significant quantification improvements can be made compared to direct calibration without matrix matching when no matrix-matched calibration standards are available. Fig. 2 shows a flowchart of the volume-normalization method for multi-point calibration although this can also be used for one-point calibration. This approach has already been used successfully for calibration in LA-ICP-MS mapping to account for variations in ablation rates between and within samples of the same matrix origin in samples that are not entirely homogenous – composite [36].

LA-ICP-MS analysis of elements in the calibration standards (Cx, with x the calibration standard number) and the sample (S) yields the gas blank-subtracted intensities $A_{Cx}$ and $A_S$ (in cps); associated ablation craters have volumes $V_{Cx}$ and $V_S$ (in μm$^{-3}$). By definition the element concentration $conc_{(S,m/V)}$ in the sample produced by this calibration

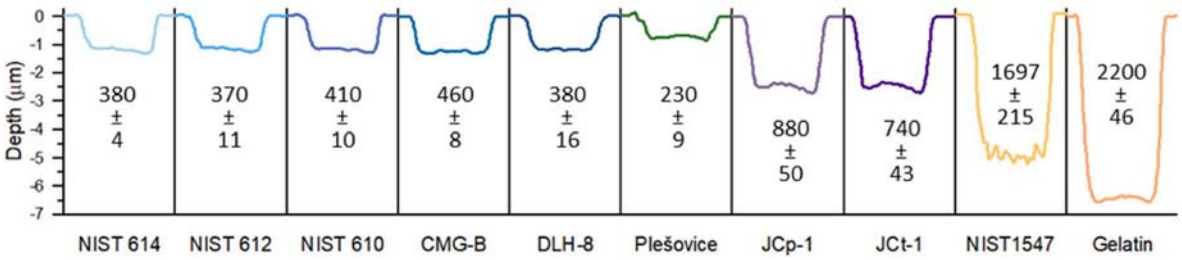


**Fig. 1.** Cross-sectional ablation crater profiles in diverse materials applying 10 cumulative laser shots per crater with a beam size of 20 μm (square mask) at a fluence of 3.6 J cm$^{-2}$; for each material the average crater volume and standard deviation (μm$^3$) is given (N = 10).

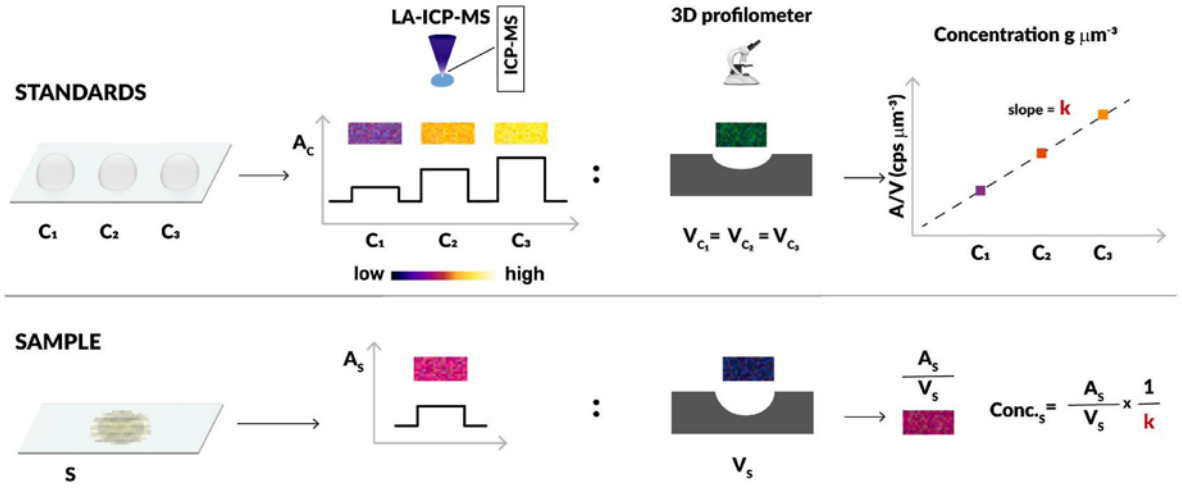


**Fig. 2.** Flowchart of the ablation volume-normalization method where sample S is subjected to multi-point calibration with calibration standards Cx (C1, C2 and C3).

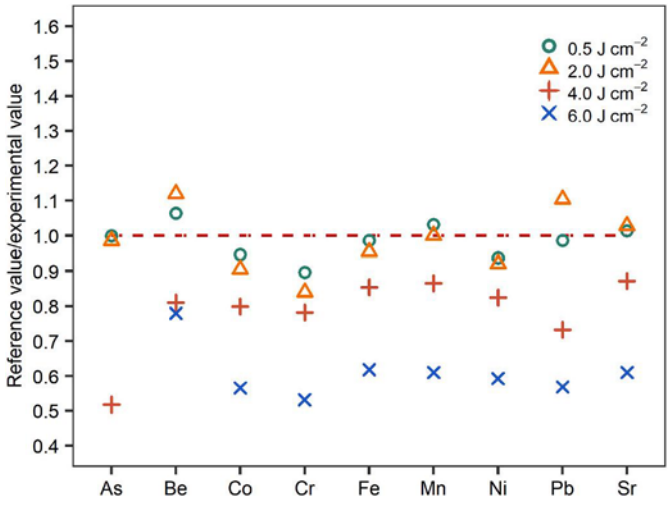


**Fig. 3.** Accuracy of the ablation-volume normalization method for LA-ICP-MS analysis of NIST 610 glass treated as a sample using custom-prepared multielement gelatin calibration standards. The NIST 610 glass was ablated at a fluence of 3.6 J $cm^{-2}$ whereas the gelatin standard underwent ablation at fluences of 0.5, 2.0, 4.0 and 6.0 J $cm^{-2}$ (further operational details can be found in Table 2). The red dashed line refers to a correct concentration determination, i.e., the concentrations measured are in agreement with the certified concentration for NIST610.

approach is in mass/volume units (µg $cm^{-3}$), calculated via

$$conc_{(S,m/V)}=(A_S/V_S)/k \quad (1)$$

where $k=(A_{Cx}/V_{Cx})/conc_{(Cx,\ m/V)}$ is the slope of the calibration graph (linear regression, forced through zero) shown in Fig. 2. This implies that the calibration standard concentrations $conc_{(Cx,m/V)} = conc_{(Cx,m/m)}\cdot D_{Cx}$ (in µg $cm^{-3}$) require knowledge of the densities $D_{Cx}$ (in µg $g^{-1}$). When the density $D_S$ (in g $cm^{-3}$) of the sample is also available, the mass/mass concentration of the sample follows from $conc_{(S,m/m)} = conc_{(S,m/V)}/D_S$ (in µg $g^{-1}$).

### 3.3. Influence of laser fluence on calibration by ablation volume-normalization

Because laser fluence impacts not only the quantity of ablated material but also the particle size distribution within the laser ablation plume, which in turn could influence particle transfer and ionization dynamics within the ICP [35,37], it is evident that optimal laser fluences exist for ablating 'hard' and 'soft' materials. We conducted a series of ablation volume-normalization experiments whereby custom-prepared multielement gelatin standards (10–250 µg $g^{-1}$) at a range of laser fluences (0.5, 2.0, 4.0, and 6.0 J $cm^{-2}$) were used to analyse NIST 610 at a fixed laser fluence of 3.6 J $cm^{-2}$.

Nine experimental concentration values obtained by treating NIST 610 glass as a sample were compared with reference concentration values (Fig. 3). Concentrations obtained from the calibration with the lowest fluence (0.5 J $cm^{-2}$) most closely matched the reference values, with deviations less than 10 %. Higher fluence values, particularly those of 4.0 and 6.0 J $cm^{-2}$, produced results that showed notable deviations from the reference values, i.e., 20 % for 4.0 J $cm^{-2}$ and >40 % for 6.0 J $cm^{-2}$. This underlines the critical role of fluence in the selection of appropriate calibration parameters, especially for "soft" materials. Therefore, it is crucial to use the most suitable fluence for each material (see Table 2 in the experimental section), i.e., slightly above the ablation threshold and associated with the highest signal-to-noise ratios [35].

### 3.4. Cross-matrix quantification via the ablation volume-normalization method in one-point calibration mode

Given the growing range of laser ablation applications, the requirement of matrix-matched calibration has become a challenge due to the limited availability of suitable reference materials. As a result, this scenario has fostered the development of various calibration methods over time, mostly with the goal of identifying suitable matrices tailored to specific samples [27]. The ablation volume-normalization method put forward here may change the calibration paradigm if accurate and precise quantification results can be obtained using a non-matrix matched calibration approach.

Validation of the ablation volume-normalization method, as outlined in Fig. 2, was carried out through cross-matrix calibration. This involved quantifying nine elements across ten distinct matrices via one-point calibration (see Table 2 for details, including an optimal ablation fluence for each of the matrices with known or measurable density), where each material was measured against every other material in bulk analysis mode, and using them both as sample and calibration standard. Heat maps in Fig. 4 display the absolute relative bias (=100 × |experimental value – recommended value|/recommended value, in %) with and without ablation-volume normalization in the cross-calibration of the nine elements (more detailed heat maps can be found in Figure S1). The heat maps indicate that the majority of the calibration standards lack certain elements, with the exception of Sr and Mn, which further emphasizes the challenge posed by matrix-matched calibration. Moreover,

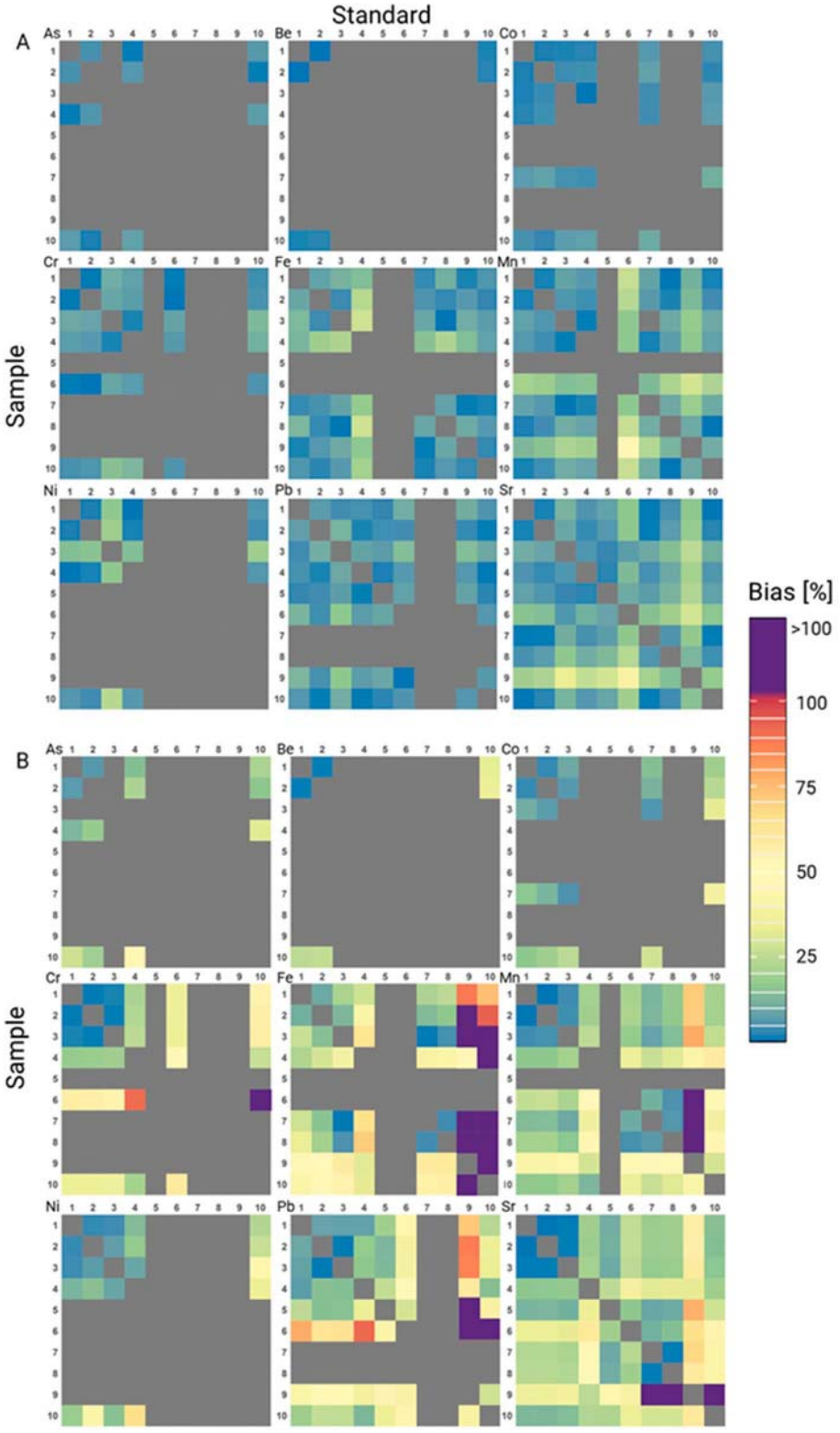


**Fig. 4.** Heat maps showing the average measurement bias by cross-calibrating nine elements (As, Be, Co, Cr, Fe, M, Ni, Pb and Sr), with (A) and without (B) ablation volume-normalization. Pixels in the maps are defined by one-point calibration standards in the columns and samples in the rows, where 1 = NIST 610, 2 = NIST 612, 3 = NIST 614, 4 = CMG-B, 5 = DLH8, 6 = Plešovice, 7 = JCp-1, 8 = JCt-1, 9 = NIST 1547, and 10 = Gelatin gel.

the superiority of data acquired through ablation-volume normalization is clearly evident compared to data obtained without employing this method.

In addition to the overall enhancement in concentration determination accuracy, Fig. 4 reveals several other important details. Fig. 4A shows that the bias in the majority of the measured concentrations with ablation volume-normalization is less than 15 %. For the less well-defined standards Plešovice and NIST 1547, a higher bias is observed in Fig. 4A for most materials. For Plešovice this is due to a lack of microscale homogeneity [33], further compounded by the potential

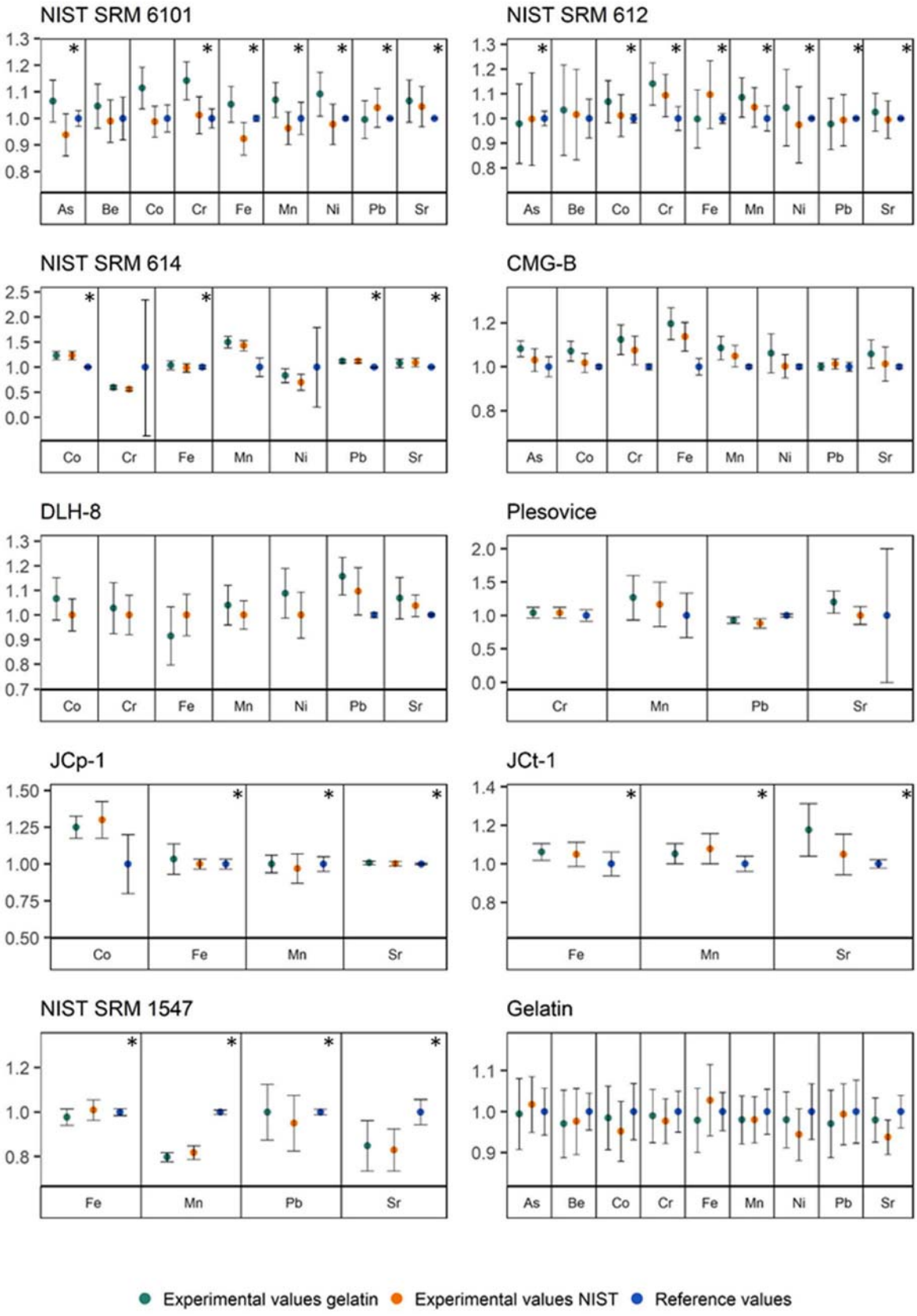


**Fig. 5.** Validation of accuracy and precision of the ablation volume-normalization method in multi-point calibration mode by comparing the concentrations obtained with the reference concentrations of up to nine elements in ten CRMs. The results are displayed as concentrations normalized to the reference concentrations, where unity values in the figure are directly linked to the reference concentrations. The error bars are representative for the standard deviations in the experimental data for the NIST 61X (5, 50 and 500 μg $g^{-1}$) and gelatin standards (10–250 μg $g^{-1}$) and the reference data, either the certified reference values in the COA (indicated with an asterisk) or the calculated values from reported concentrations in the GeoRem database (for the missing elements).

inaccuracy of the reported density [34] used in the calculations, whereas for NIST 1547 pelletizing issues associated with the hydraulic pressure might be the culprit. As expected, quantification data without ablation volume-normalization in Fig. 4B show a much higher bias, and only were matrices of standard and sample exactly match, e.g., for the NIST 61X glasses or the two carbonate materials - JCt, JCp lower bias values can be observed. The latter confirms the LA-ICP-MS prerequisite, that for the accurate quantitative work a matrix matched standard is obligatory in the conventional way, whereas in the proposed approach a well-defined (certified) standard can be used for quantification of any other material. However, even when using a matrix-matched standard, care must be taken if the sample is not homogeneous, as differences may occur during the ablation of the same sample, hence making an accurate quantification impossible without volume normalization [36].

### 3.5. Accuracy and precision of the ablation volume-normalization method in multi-point calibration mode

The versatility of the proposed method gains further significance when one can locate commercial or custom-prepared multielement standards across various concentration levels. This enables the execution of multi-point calibration, and thus establishment of a slope (see Fig. 2), instead of one-point calibration used in Fig. 4. Candidates for such calibration standards are i) the NIST 61X standards, having similar main matrix compositions (comparable concentrations of $SiO_2$, $Na_2O$, $Al_2O_3$, and CaO, which make up more than 96 % of the matrices), but variable minor and trace element concentrations, and ii) the custom-prepared gelatin standards with the flexibility to span the necessary concentration range for any element required, particularly in the context of biomedical mapping where standard references are typically unavailable.

In Fig. 5 (Table S1 gives the actual concentrations associated with this figure) it is visually demonstrated that in the absence of matrix-matched standards, the ablation volume-normalization method can generate accurate and precise data using the NIST 61X standards (5, 50 and 500 μg $g^{-1}$) or the custom-prepared gelatin standards (10–250 μg $g^{-1}$) using multi-point calibration for measurement of up to nine elements in ten standard reference matrices. Even though only a portion (ca. 47 %) of the nine elements selected are certified in all reference materials (elements with an asterisk in Fig. 5), the missing data were "filled in" by unweighted averaging of the element concentrations reported in the GeoReM database for the individual elements [38,39]. The error bars are representative for the standard deviations in i) the experimental data for the NIST 61X and gelatin standards (N = 5), and ii) the reference data, either the certified reference values (after recalculation from expanded uncertainties in the COA), or the calculated values from reported concentrations in the GeoRem database (for the missing elements). From Fig. 5 we can see that in all cases the experimental uncertainties obtained with the ablation volume-normalization method are closely matching the uncertainties of the reference data.

While the gelatin standards are very easy to work with (*i.e.* good crater shapes, low energy, easy to focus …), allow the addition of any element in a wide concentration range, the NIST 61X glass standards are readily available, certified, widely used and easy to work with. Despite extrapolating the concentrations of certain elements in specific samples from the calibration curve's range, these findings remained consistent with the certified values of the CRMs. This agreement was due to the broad linear range of ICP-MS and the adoption of a calibration curve, which alleviated the potential adverse impact of a single measurement error on the calibration slope. This situation could arise when employing a one-point calibration, a common practice in LA-ICP-MS measurements, primarily because suitable matrix-matched standards are often unavailable, especially in the diverse range necessary to construct a comprehensive calibration curve.

## 4. Conclusions

The utilization of commonly accessible certified reference materials (CRMs), such as NIST 61X glasses, is generally limited to samples sharing a similar matrix composition. This limitation hinders their applicability in accurately quantifying elements if e.g. biological samples, which lack widely accepted CRMs and instead resort to custom-prepared standards. In this investigation, we present a calibration technique for LA-ICP-MS that eliminates the necessity for matrix-matching. This pioneering method holds great potential across various fields and offers a simplified quantification solution for scenarios where traditional certified reference materials are unavailable.

Our approach, involving ablation-volume normalization, underwent thorough assessment across diverse material types including glass (NIST SRM 610, NIST SRM 612, NIST SRM 614, CMG-B, DLH-8), carbonates (JCp-1, JCt-1), plant specimens (NIST SRM 1547), zircons (Plešovice), and proteinaceous substances (gelatin). The quantified concentrations for all materials consistently matched certified values, effectively showcasing the transferability of calibration standards among materials with well-defined elemental compositions. Notably, gelatin and glass demonstrated remarkable suitability. Discrepancies in elemental concentration determinations mostly remained below 10 %, except in cases of exceedingly low concentrations.

In stark contrast to the conventional LA-ICP-MS calibration dependent on matrix-matched standards, our innovative methodology introduces a more robust calibration procedure that remains effective even when such standards are unavailable. This groundbreaking advancement holds the potential to enhance the accuracy and precision of elemental analysis through LA-ICP-MS, spanning a wide array of research applications.

## CRediT authorship contribution statement

**Kristina Mervič:** Data curation, Formal analysis, Software, Validation, Visualization, Writing – original draft, Writing – review & editing. **Vid S. Šelih:** Conceptualization, Writing – review & editing. **Martin Šala:** Conceptualization, Funding acquisition, Investigation, Methodology, Resources, Supervision, Validation, Writing – original draft, Writing – review & editing. **Johannes T. van Elteren:** Conceptualization, Methodology, Validation, Writing – review & editing.

## Declaration of competing interest

The authors declare that they have no known competing financial interests or personal relationships that could have appeared to influence the work reported in this paper.

## Data availability

Data will be made available on request.

## Acknowledgment

The authors acknowledge the financial support from the Slovenian Research Agency ARRS research core funding no. P1-0034. K.M. thanks the Slovenian Research Agency ARRS for funding her PhD research.

## Appendix A. Supplementary data

Supplementary data to this article can be found online at https://doi.org/10.1016/j.talanta.2024.125712.

## References

[1] D. Chew, K. Drost, J.H. Marsh, J.A. Petrus, LA-ICP-MS imaging in the geosciences and its applications to geochronology, Chem. Geol. 559 (2021) 119917.

[2] J. Almirall, A. Akmeemana, K. Lambert, P. Jiang, E. Bakowska, R. Corzo, C. M. Lopez, E.C. Pollock, K. Prasch, T. Trejos, P. Weis, W. Wiarda, H. Xie, P. Zoon, Determination of seventeen major and trace elements in new float glass standards for use in forensic comparisons using laser ablation inductively coupled plasma mass spectrometry, Spectrochim. Acta, Part B 179 (2021) 106119.

[3] Q. Li, Z. Wang, J. Mo, G. Zhang, Y. Chen, C. Huang, Imaging gold nanoparticles in mouse liver by laser ablation inductively coupled plasma mass spectrometry, Sci. Rep. 7 (1) (2017) 2965.

[4] R. Luo, X. Su, W. Xu, S. Zhang, X. Zhuo, D. Ma, Determination of arsenic and lead in single hair strands by laser ablation inductively coupled plasma mass spectrometry, Sci. Rep. 7 (1) (2017) 3426.

[5] H.R. Ali, H.W. Jackson, V.R.T. Zanotelli, E. Danenberg, J.R. Fischer, H. Bardwell, E. Provenzano, C.I.G.C. Team, O.M. Rueda, S.F. Chin, S. Aparicio, C. Caldas, B. Bodenmiller, Imaging mass cytometry and multiplatform genomics define the phenogenomic landscape of breast cancer, Nat. Cancer. 1 (2) (2020) 163–175.

[6] P.A. Doble, R.G. de Vega, D.P. Bishop, D.J. Hare, D. Clases, Laser ablation-inductively coupled plasma-mass spectrometry imaging in biology, Chem. Rev. (2021) 11769–11822.

[7] T. Ubide, B.S. Kamber, Volcanic crystals as time capsules of eruption history, Nat. Commun. 9 (1) (2018) 326.

[8] C. Giesen, H.A.O. Wang, D. Schapiro, N. Zivanovic, A. Jacobs, B. Hattendorf, P. J. Schüffler, D. Grolimund, J.M. Buhmann, S. Brandt, Z. Varga, P.J. Wild, D. Günther, B. Bodenmiller, Highly multiplexed imaging of tumor tissues with subcellular resolution by mass cytometry, Nat. Methods 11 (4) (2014) 417–422.

[9] T. Van Acker, S. Theiner, E. Bolea-Fernandez, F. Vanhaecke, G. Koellensperger, Inductively coupled plasma mass spectrometry, Nat. Rev. Methods Primers 3 (1) (2023) 53.

[10] T. Van Acker, S.J.M. Van Malderen, T. Van Helden, C. Stremtan, M. Šala, J.T. van Elteren, F. Vanhaecke, Analytical figures of merit of a low-dispersion aerosol transport system for high-throughput LA-ICP-MS analysis, J. Anal. Atom. Spectrom. 36 (6) (2021) 1201–1209.

[11] S.J.M. Van Malderen, J.T. van Elteren, F. Vanhaecke, Development of a fast laser ablation-inductively coupled plasma-mass spectrometry cell for sub-μm scanning of layered materials, J. Anal. Atom. Spectrom. 30 (1) (2015) 119–125.

[12] A. Gundlach-Graham, M. Burger, S. Allner, G. Schwarz, H.A. Wang, L. Gyr, D. Grolimund, B. Hattendorf, D. Gunther, High-speed, high-resolution, multielemental laser ablation-inductively coupled plasma-time-of-flight mass spectrometry imaging: part I. Instrumentation and two-dimensional imaging of geological samples, Anal. Chem. 87 (16) (2015) 8250–8258.

[13] G. Craig, A.J. Managh, C. Stremtan, N.S. Lloyd, M.S.A. Horstwood, Doubling sensitivity in multicollector ICPMS using high-efficiency, rapid response laser ablation technology, Anal. Chem. 90 (19) (2018) 11564–11571.

[14] J.T. van Elteren, V.S. Šelih, M. Šala, Insights into the selection of 2D LA-ICP-MS (multi)elemental mapping conditions, J. Anal. Atom. Spectrom. 34 (9) (2019) 1919–1931.

[15] J.T. van Elteren, D. Metarapi, M. Šala, V.S. Šelih, C.C. Stremtan, Fine-tuning of LA-ICP-QMS conditions for elemental mapping, J. Anal. Atom. Spectrom. 35 (11) (2020) 2494–2497.

[16] M. Šala, V.S. Šelih, C.C. Stremtan, T. Tămaş, J.T. van Elteren, Implications of laser shot dosage on image quality in LA-ICP-QMS imaging, J. Anal. Atom. Spectrom. 36 (1) (2021) 75–79.

[17] O.B. Bauer, O. Hachmöller, O. Borovinskaya, M. Sperling, H.-J. Schurek, G. Ciarimboli, U. Karst, LA-ICP-TOF-MS for rapid, all-elemental and quantitative bioimaging, isotopic analysis and the investigation of plasma processes, J. Anal. Atom. Spectrom. 34 (4) (2019) 694–701.

[18] M. Burger, G. Schwarz, A. Gundlach-Graham, D. Käser, B. Hattendorf, D. Günther, Capabilities of laser ablation inductively coupled plasma time-of-flight mass spectrometry, J. Anal. Atom. Spectrom. 32 (10) (2017) 1946–1959.

[19] M. Vázquez Peláez, J.M. Costa-Fernández, A. Sanz-Medel, Critical comparison between quadrupole and time-of-flight inductively coupled plasma mass spectrometers for isotope ratio measurements in elemental speciation, J. Anal. Atom. Spectrom. 17 (8) (2002) 950–957.

[20] M. Balcerzak, An overview of analytical applications of time of flight-mass spectrometric (TOF-MS) analyzers and an inductively coupled plasma-TOF-MS technique, Anal. Sci. 19 (7) (2003) 979–989.

[21] D. Günther, C.A. Heinrich, Comparison of the ablation behaviour of 266 nm Nd: YAG and 193 nm ArF excimer lasers for LA-ICP-MS analysis, J. Anal. Atom. Spectrom. 14 (9) (1999) 1369–1374.

[22] I. Kroslakova, D. Günther, Elemental fractionation in laser ablation-inductively coupled plasma-mass spectrometry: evidence for mass load induced matrix effects in the ICP during ablation of a silicate glass, J. Anal. Atom. Spectrom. 22 (1) (2007) 51–62.

[23] H.P. Longerich, D. Günther, S.E. Jackson, Elemental fractionation in laser ablation inductively coupled plasma mass spectrometry, Fresenius' J. Anal. Chem. 355 (5) (1996) 538–542.

[24] M. Guillong, D. Günther, Effect of particle size distribution on ICP-induced elemental fractionation in laser ablation-inductively coupled plasma-mass spectrometry, J. Anal. Atom. Spectrom. 17 (8) (2002) 831–837.

[25] H. Pan, L. Feng, Y. Lu, Y. Han, J. Xiong, H. Li, Calibration strategies for laser ablation ICP-MS in biological studies: a review, TrAC, Trends Anal. Chem. 156 (2022) 116710.

[26] M. Martinez, M. Baudelet, Calibration strategies for elemental analysis of biological samples by LA-ICP-MS and LIBS – a review, Anal. Bioanal. Chem. 412 (1) (2020) 27–36.

[27] A. Limbeck, P. Galler, M. Bonta, G. Bauer, W. Nischkauer, F. Vanhaecke, Recent advances in quantitative LA-ICP-MS analysis: challenges and solutions in the life sciences and environmental chemistry, Anal. Bioanal. Chem. 407 (22) (2015) 6593–6617.

[28] J. Cizdziel, K. Bu, P. Nowinski, Determination of elements in situ in green leaves by laser ablation ICP-MS using pressed reference materials for calibration, Anal. Methods 4 (2) (2012) 564–569.

[29] A. Schweikert, S. Theiner, M. Šala, P. Vician, W. Berger, B.K. Keppler, G. Koellensperger, Quantification in bioimaging by LA-ICPMS - evaluation of isotope dilution and standard addition enabled by micro-droplets, Anal. Chim. Acta 1223 (2022) 340200.

[30] M. Šala, V.S. Šelih, J.T. van Elteren, Gelatin gels as multi-element calibration standards in LA-ICP-MS bioimaging: fabrication of homogeneous standards and microhomogeneity testing, Analyst 142 (18) (2017) 3356–3359.

[31] A. Schweikert, S. Theiner, D. Wernitznig, A. Schoeberl, M. Schaier, S. Neumayer, B. K. Keppler, G. Koellensperger, Micro-droplet-based calibration for quantitative elemental bioimaging by LA-ICPMS, Anal. Bioanal. Chem. 414 (1) (2022) 485–495.

[32] Calibration standards for microanalysis. https://www.my-standards.com/, 2023. (Accessed 4 April 2023).

[33] J. Sláma, J. Košler, D.J. Condon, J.L. Crowley, A. Gerdes, J.M. Hanchar, M.S. A. Horstwood, G.A. Morris, L. Nasdala, N. Norberg, U. Schaltegger, B. Schoene, M. N. Tubrett, M.J. Whitehouse, Plešovice zircon — a new natural reference material for U–Pb and Hf isotopic microanalysis, Chem. Geol. 249 (1) (2008) 1–35.

[34] Zircon Mineral Data. http://webmineral.com/data/Zircon.shtml#.Y7UsK9XMKUk. (Accessed 29.September 2023).

[35] A. Jerše, K. Mervič, J.T. van Elteren, V.S. Šelih, M. Šala, Quantification anomalies in single pulse LA-ICP-MS analysis associated with laser fluence and beam size, Analyst 147 (23) (2022) 5293–5299.

[36] K. Mervič, J.T. van Elteren, M. Bele, M. Šala, Utilizing ablation volume for calibration in LA-ICP-MS mapping to address variations in ablation rates within and between matrices, Talanta (2023) 125379.

[37] S. Zhang, M. He, Z. Yin, E. Zhu, W. Hang, B. Huang, Elemental fractionation and matrix effects in laser sampling based spectrometry, J. Anal. Atom. Spectrom. 31 (2) (2016) 358–382.

[38] K. Jochum, U. Nohl, K. Herwig, E. Lammel, B. Stoll, A. Hofmann, GeoReM: a new geochemical database for reference materials and isotopic standards, Geostand. Geoanal. Res. 29 (2007) 333–338.

[39] GeoReM - Database on geochemical and environmental reference materials. http://georem.mpch-mainz.gwdg.de/. (Accessed 29.September. 2023).